Cockroach-inspired winged robot reveals principles of ground-based dynamic self-righting

Chen Li[1*], Chad C. Kessens[2], Austin Young[3], Ronald S. Fearing[3], and Robert J. Full[3]

Abstract— **Animals and robots alike face challenges of flipping-over as they move in complex terrain. Small insects like cockroaches can rapidly right themselves when upside down, yet small fast-running legged robots are much less capable of ground-based self-righting. Inspired by the discoid cockroach that opens its wings to push against the ground to self-right, we designed actuated wings for robot self-righting based on recently-developed rounded shells for obstacle traversal [1]. We measured the self-righting performance of a robot using these actuated wings, and systematically studied the effects and trade-offs of wing opening magnitude, speed, symmetry, and wing geometry. Our study provided a proof-of-concept that robots can take advantage of an existing body structure (rounded shell) in novel ways (as actuated wings) to serve new locomotor functions, analogous to biological exaptations [2]. Our results demonstrated that the robot self-rights dynamically, with active wing pushing followed by passive falling, and benefits from increasing kinetic energy by pushing faster and longer. Our experiments also showed that opening both wings asymmetrically increases righting probability at low wing opening magnitudes.**

I. INTRODUCTION

Robots are on the verge of venturing into the real-world to aid humans in the performance of important tasks, such as environmental monitoring, reconnaissance, search and rescue, and extra-terrestrial exploration. In doing so, they must move through complex terrain such as desert, forest floor, building rubble and debris, and the Martian surface. Because these surfaces are often uneven [3], sloped [4], dispersed [5], cluttered [1], or even flowable [6], robots can frequently suffer static and dynamic instability, rotational perturbations, loss of foothold, and inability to generate appropriate ground reaction forces, all of which pose risks for flipping-over and losing mobility [7]. Therefore, ground self-righting capability is critical for effective locomotion and continual operation of robots.

Small, fast-running legged robots, such as RHex [3], iSprawl [8], and VelociRoACH [9], are particularly susceptible to flipping-over, because they experience large dynamic instabilities due to small body inertia [9] and terrain irregularities often comparable or even larger than themselves [10]. These robots often have relatively short, springy legs with stiffness, power, and torque capabilities tuned to generate a dynamically stable running motion [3], [8], [9], which are often less useful for self-righting. As a result, these robots either are not able to self-right, or must rely on energy storage and release mechanisms to perform aerobatics to self-right [11] [12].

To overcome the challenge of flipping-over, a variety of ground-based self-righting mechanisms have been developed, such as passively unstable body shape with low center of mass [13] [14] [15], movable center of mass [14], reconfigurable wheels [16] and tracks [17], long manipulator arms, levers, or legs [13], [18], [19], [20], spring-based legs [21], active tails [22], and self-reassembly [23], [24]. However, few of these mechanisms have been implemented on small, fast-running legged robots, largely due to their limited payload. Some small legged robots work around the problem of ground-based self-righting by adopting a dorsoventrally symmetrical body design [11], [25] or one with no "upright" orientation [26]. However, many tasks still require a nominal upright orientation [11].

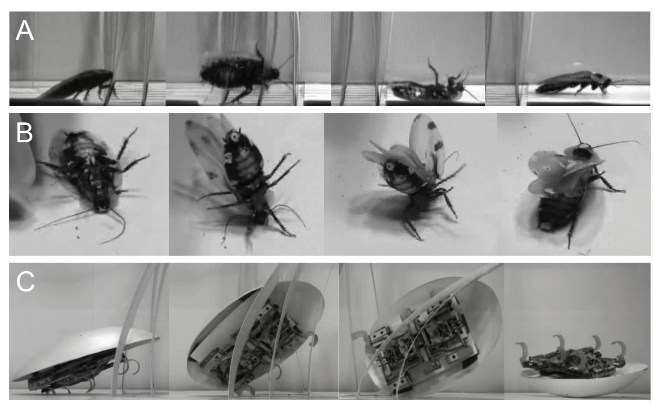

Fig. 1. Animals like insects are better than small fast-running legged robots at overcoming the challenge of flipping-over during locomotion. (A) The discoid cockroach can almost always self-right quickly after flipping-over when traversing dense obstacles such as grass-like beams [1]. (B) It does so by opening its wings to push against the ground [27]. (C) A robot with a cockroach-inspired rounded shell can traverse dense obstacles, but never self-rights if flipped-over [1].

To self-right from an upside-down orientation, many animals use **exaptations** [2] of appendages primarily used for other purposes [28], [29], [30], [31], [32]. For example, the flightless discoid cockroach have wings that are normally closed against the body to form a rounded shell to provide protection and facilitate obstacle traversal [1] (Fig. 1A).

This work is supported by Burroughs Wellcome Fund Career Award at the Scientific Interface (C.L.), Miller Institute for Basic Research in Science, University of California, Berkeley (C.L.), and United States Army Research Laboratory under the Micro Autonomous Science and Technology Collaborative Contract (C.C.K., R.J.F).

[1]Chen Li is with Johns Hopkins University, Baltimore, MD 21218, USA
[2]Chad C. Kessens is with the United States Army Research Laboratory, Aberdeen Proving Ground, MD 21005, USA
[3]Austin Young, Ronald S. Fearing, and Robert J. Full are with University of California, Berkeley, CA 94720, USA
*Author for correspondence: chen.li@jhu.edu http://li.me.jhu.edu

When flipped over, the cockroach can rapidly right itself by opening its wings and pushing them against the ground (Fig. 1B) [27]. In a previous study, we enabled a small legged robot, VelociRoACH, to traverse dense obstacles such as grass-like beams, by adding a cockroach-inspired rounded shell to facilitate body roll and reduce terrain resistance when pushing through obstacle gaps [1] (Fig. 1C). However, the rounded shell also rendered the robot trapped in a stable upside-down orientation if flipped over (Fig. 1C) [1].

We were inspired by the remarkable ability of insects to use the same body structure for multiple functions. In this paper, we further developed the rounded shell [1] into actuated wings to serve the novel function of ground self-righting. We designed a novel two degree-of-freedom joint and four-bar linkage transmissions to enable the wings to be opened in a similar fashion as those of the cockroach. We calibrated the motor output to ensure that body weight and inertial force did not affect wing actuation during righting. We then tested whether our cockroach-inspired actuated wings could enable self-righting, and systematically explored how wing opening magnitude and speed affect righting performance. We applied a geometric modeling framework [18], [33] to assess whether quasi-static righting is possible and examine the role of wing shape on kinematic and energetic requirement for dynamic self-righting, and used a simple dynamic model to understand the passive falling dynamics during self-righting. Finally, we tested the robot with differential left and right wing actuation to understand the advantage of asymmetric wing opening for self-righting [27].

II. RIGHTING MECHANISM DEVELOPMENT

A. Design of Actuated Wings

The morphology and kinematics of the wings for self-righting (Fig. 2) were inspired from those of the discoid cockroach (Fig. 1B). We used the same ellipsoidal shell (18 cm long, 12 cm wide, 3 cm tall) previously developed for obstacle traversal [1], and sliced it in half to form two wings (Fig. 2A,B). To allow the robot wings to move in a similar fashion to those of the cockroach (Fig. 1B), we developed a two degree-of-freedom (DoF) joint (Fig. 2C) using the Smart Composite Microstructure fabrication technique [34] and a four-bar linkage transmission (Fig. 2D). When fully closed, the dorsal surface of the two robot wings formed a rounded shell, similar to the animal. The 2-DoF joint connected the wings to the front end of the body. The first degree of freedom allowed the wing base to pitch relative to the body (Fig. 2D). The second degree of freedom allowed the wings to roll about to the midline of the wing base (Fig. 2E). The two servo motors that open the two wings could be actuated by either using the same control signal (symmetric wing opening) or independently (asymmetric wing opening).

Wings were actuated by small, lightweight, high-torque servo motors (Hyperion DS11-AMB). The transmission of each wing was composed of a 3D-printed link, two heim joints, and two steel rods. The flexibility of the thermo-formed wings and slight rotation, twisting, and flexion present between parts allowed the wings to open to a larger

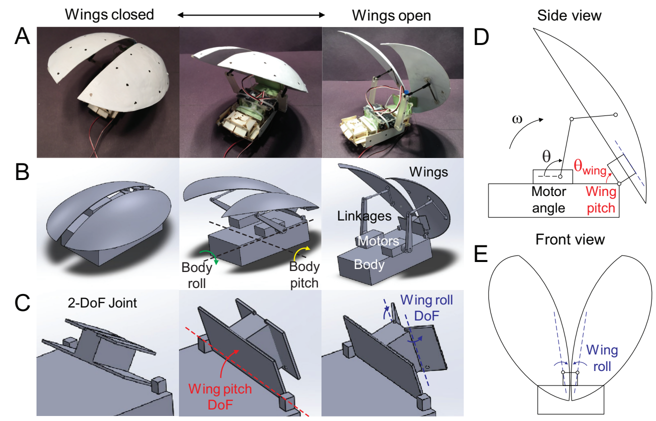

Fig. 2. Design of actuated wings for self-righting. (A) Photos of the actuated wings on a VelociRoACH robot body, from closed to open configurations. (B) CAD design of the self-righting mechanism. (C) CAD design of the two degree-of-freedom joint. (D) Diagram showing the first degree of freedom, wing pitch, *via* a four bar linkage transmission. (E) Diagram showing the second degree of freedom, wing roll.

extent than if wings were rigid and if the entire transmission were constrained to move in the sagittal plane. A string restricted the range of wing pitch to within 75° from the body.

Because our study focused on achieving and understanding self-righting using wings, we used a VelociRoACH robot body (11 cm long, 6.5 cm wide, 3 cm tall) without legs. The total weight of the robot including body, wings, motors, and transmissions was 100 g, with about half the weight in the motors and transmissions. Solidworks modeling of the robot showed that the center of mass was close to the body geometric center, similar to that of the animal. Fine cables provided constant power and control signals, and were routed through the gap between the two wings at the front end of the robot to minimize drag force during self-righting and interference with wing actuation. Custom electronics (Arduino Pro Mini V13) and software controlled the motor actuation.

B. Calibration of Motor Actuation

To assess whether the robot's body weight and ground reaction force during self-righting significantly affected wing actuation, we performed experiments to calibrate the servo motors. We took high-speed videos (100 frame/s) of the robot opening its wings, both in an upright orientation with the body fixed to the ground, and starting from the upside-down orientation in an attempt to self-right. We tracked markers on the body and wing transmission from side view videos and measured the motor angle, θ (the angle by which the motor rotated) and average motor speed*, ω, and compared them to motor input command (Fig. 3). We found that motor angle θ was most accurate between 80° and 140° (Fig. 3A),

*We verified that the motor was fast in accelerating and decelerating to desired speeds so that the majority (≈ 90%) of rotation occurred at a nearly constant speed. Thus we simply used the average angular velocity to represent motor speed, assuming instantaneous acceleration and deceleration.

and that motor speed ω was accurate up to 250°/s (Fig. 3B). In addition, the added body weight and inertial force during self-righting had little effect on motor actuation.

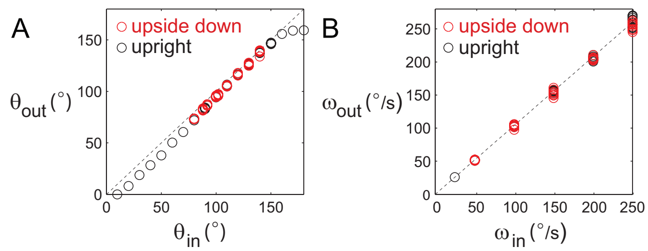

Fig. 3. Comparison of (A) angle and (B) speed of motor output to motor input. Black: upright; red: upside down. Diagonal lines indicate perfect motor output.

III. SYMMETRIC RIGHTING EXPERIMENTS

A. Righting via Symmetric Wing Opening

As a first step to test whether and how well the robot can self-right using wings, we chose to perform experiments on a flat, level, rigid surface. We positioned the robot upside down with the wings fully closed, and opened both wings in synchrony (symmetric wing opening) with the same motor angle θ and speed ω. We used high speed video to record the robot's self-righting attempts from both top and side (Fig. 4A) views, and tracked markers on the robot body from the side view to measure the body pitch angle, θ_{body}, and calculated body angular velocity, ω_{body}.

Similar to the discoid cockroach, the robot body pitched up as it opened both wings and pushed them against the ground. As the body continued to pitch, it vaulted over the front edge of the wings (analogous to the head of the cockroach) and successfully righted, with a change of body pitch angle θ_{body} from $-80\,°$ to 90° (Fig. 4B, see attached video). Because the robot did not close wings after wing opening, failed attempts resulted in the body settling into a vertical orientation ($\theta_{body} \approx 0$, see attached video).

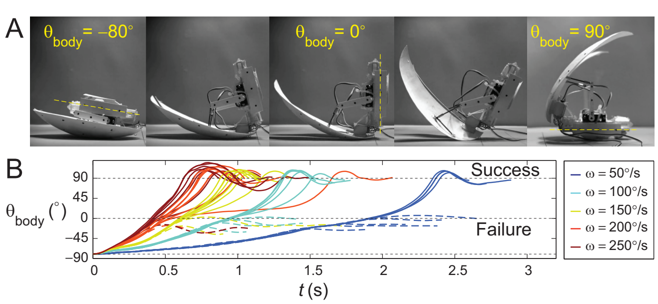

Fig. 4. Body rotation of the robot during self-righting. (A) Snapshots of the robot during successful self-righting, with definition of body pitch angle θ_{body}. (B) θ_{body} as a function of time, t, for various motor speeds ω and angle θ. Trials of the same color use the same ω but different θ. Solid and dashed curves indicate successful and failed trials.

B. Effect of Wing Opening Magnitude & Speed

To discover principles of self-righting using symmetric wing opening, we tested how wing opening magnitude and speed affected the robot's performance (Fig. 5) including righting probability, P_{right} (success = 1, failure = 0), and righting time, t_{right}.

Although wing pitch angle θ_{wing} does not equal motor angle θ due to the four-bar linkage transmission (Fig. 2D), within the range of motor angle θ tested in righting experiments ($\leq$ 140°), θ_{wing} increases monotonically with θ (and thus ω_{wing} increases monotonically with ω). Thus, we used θ and ω as a proxy to test the effect of wing opening magnitude and speed. Both θ and ω were varied within the range of high motor fidelity: 80° $\leq \theta \leq$ 140° (which corresponded to 45° $\leq \theta_{wing} \leq$ 75°), 0°/s $\leq \omega \leq$ 250°/s. Preliminary experiments showed excellent repeatability for all θ and ω tested (s.d. of $t_{right} <$ 0.1 s), thus we performed one high-speed video trial for each combination of θ and ω.

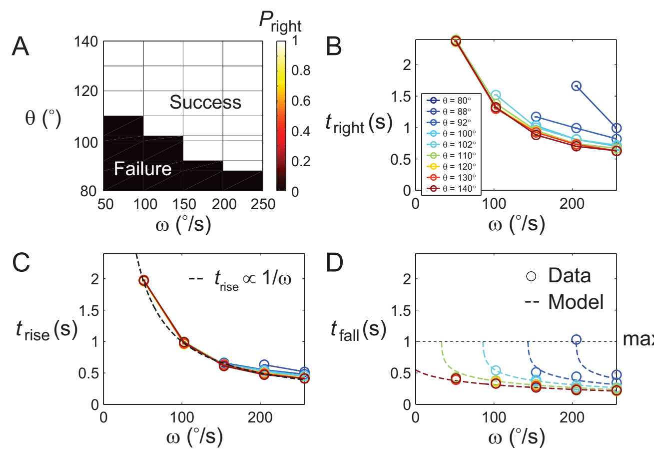

Fig. 5. Robot righting performance is sensitive to wing opening magnitude and speed. (A) Righting probability (success = 1, failure = 0) as a function of motor angle θ and speed ω. (B) Righting time, (C) rising time, and (D) falling time as a function of ω for a range of θ. In (B)-(D), redder colors indicate higher θ and bluer colors indicate lower θ. In (D), dashed curves are fits from the dynamic model (Fig. 8, Section IV B).

We found that increasing θ and increasing ω both increased the robot's righting probability (Fig. 5A). When θ was sufficiently high ($>$ 110°), the robot always righted even with the lowest ω tested; when θ was sufficiently low ($<$ 88°), the robot always failed to right even at the highest ω tested. For intermediate θ (88° $\leq \theta \leq$ 110°), the robot righted at high ω but failed at low ω. Besides increasing righting probability, increasing θ and ω also both made righting faster. For any given θ, t_{right} decreased with ω; for any given ω, t_{right} also decreased with θ (Fig. 5B). These results demonstrated that the more and faster the wings open, the more successful and quicker it is for the robot to self-right.

To better understand the righting process, we further examined the time for the robot body to rise from the upside-down orientation to a vertical orientation, t_{rise}, and the subsequent time for it to fall to the upright orientation, t_{fall}. We found that t_{rise} was almost always inversely proportional to ω, and differed little when θ changed (Fig. 5C). By contrast, t_{fall} decreased with ω for any given θ, and decreased with θ for any given ω (Fig. 5D, circles).

IV. SYMMETRIC RIGHTING MODELING

A. Geometric Modeling

To understand whether the robot is capable of quasi-static self-righting or must right dynamically, we applied a generic planar self-righting analysis framework [18] and self-rightability metric [33]. Because the roll motion of the wings did not substantially change the projected wing shape in the sagittal plane (except for large motor angles), we approximated the sagittal wing shape as a rigid truncated ellipse (Fig. 6A). To explore the effect of wing geometry, we constrained wing length L and truncation distance D and varied wing height ϵL, where ϵ is wing height normalized to wing length (for the robot used in experiments, L = 18 cm and D = 13 cm). Semi-major axis a was variable but determined for any given ϵ. Body and wing dimensions, center of mass positions, and body-wing joint position (Fig. 6B) were determined from the robot used in experiments.

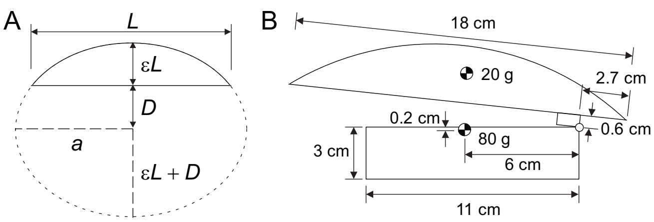

Fig. 6. (A) Truncated elliptical model of the wings in the sagittal plane with geometric variables (wing height ϵL, semi-major axis a) and constraints (wing length L and truncation distance D). (B) Planar geometric model of the robot.

Using the geometric framework [18], we examined how the minimal wing pitch angle, θ_{wing}^{req}, required to guarantee self-righting using quasi-static wing actuation (Fig. 7A) depended on wing height (see Fig. 7C for examples). This would be necessary if, for example, a joint were highly geared and unable to generate angular velocities that might be required for dynamic righting. We found that wing geometry had a significant impact on θ_{wing}^{req}. For less tall wings ($\epsilon \leq 0.13$), θ_{wing}^{req} was above 120° and changed little with ϵ. As wings became taller ($\epsilon > 0.13$), θ_{wing}^{req} quickly decreased with ϵ. In particular, for the robot used in experiments with ϵ = 0.17 (Fig. 7A, vertical line), the model predicted that $\theta_{wing}^{req} \approx 90°$. This means that kinetic energy would be required if θ_{wing} could not reach 90°. Because the robot used in experiments was only capable of $\theta_{wing} \leq 75°$ (Fig. 7A, white region), it must be righting dynamically†. More broadly, the negative dependence of θ_{wing}^{req} on ϵ also suggests that, for quasi-static self-righting, an inability of the robot (or animal) to open wings to larger wing pitch angles can be compensated by having taller wings, and having less tall wings can be compensated by adopting a larger range of wing pitch motion.

To understand the energetic requirements of dynamic self-righting, we constrained θ_{wing} to be $\leq$ 75° (based on the robot used in experiments) and calculated the minimal potential energy barrier, ΔE, which the robot must overcome to self-right from the stable upside-down orientation with wings closed. We found that ΔE decreased with ϵ (Fig. 7B, solid curve), demonstrating that tall wings are energetically more advantageous by saving the mechanical energy needed for dynamic righting. In addition, compared to one with actuated wings, a robot with static, closed wings (Fig. 7B, dashed curve) had to overcome a much higher ΔE, e.g., by $\sim 10\times$ for the robot used in experiments with ϵ = 0.17 (vertical line). This suggests that animals save energy by using wings to self-right compared to passive righting using rigid shells (e.g., turtles with highly-domed shells [30]).

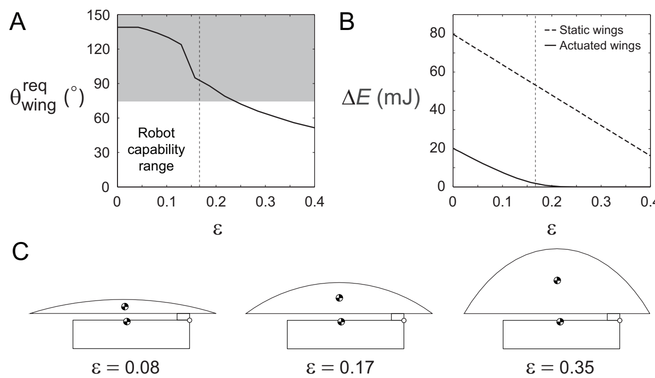

Fig. 7. (A) Minimal wing pitch angle required for quasi-static self-righting as a function of normalized wing height ϵ. (B) Minimal potential energy barrier that the robot must overcome to self-right from the stable upside-down orientation with wings closed. Solid: if the robot can actuate wings. Dashed: if wings are static relative to the body. (C) Schematics of the robot geometric model with three representative wing heights. Vertical lines in (A) and (B) and the middle panel in (C) correspond with ϵ = 0.17, the value of the robot used in experiments.

These results also provide insights into the role of wing shape for biological self-righting using wings. The discoid cockroach has less tall wings ($\epsilon \approx 0.08$), which results in $\theta_{wing}^{req} > 90°$. While the animal is capable of opening wings to achieve $\theta_{wing} \approx 90°$, the θ_{wing} observed in our animal experiments were mostly lower [27]. This suggests that the animal also self-rights dynamically. In addition, the animal's less tall wings are not the most beneficial if minimizing energetic cost is the only goal. Other functions and constraints may also play an important role in the evolution of wing shape, such as protection and obstacle traversal [1]. For robots to achieve multiple locomotor functions like animals (e.g., integrating actuated wings for self-righting with shells for obstacle traversal [1]), such trade-offs should be considered.

B. Dynamic Modeling

In both our animal [27] and robot studies of self-righting using wings, wings were held almost stationary relative to the body until the animal or robot fully righted. Thus we hypothesized that body rotation dynamics during the falling phase was governed by gravity.

To test this hypothesis, we developed a simple planar dynamic model of a rigid body rotating under gravity about

†We verified that the slight deformation of wing shape due to the roll motion of the wings at large θ did not change this prediction.

a fixed pivot on the ground in the sagittal plane (Fig. 8A). This is a reasonable approximation of the robot because, for righting using symmetric wing opening, body rotation was almost exclusively within the sagittal plane, and no slip and little rolling occurred at the ground contact point during the falling phase. We used Lagrangian method to derive the equation of motion:

$$\frac{\mathrm{d}\omega_{body}}{\mathrm{d}t} = \frac{mgL\sin\theta_{body}}{I_{pitch} + mL^2} \quad (1)$$

where θ_{body} is body pitch angle, $\omega_{body} = \frac{d\theta_{body}}{dt}$ is body pitch angular velocity, t is time, m = 0.1 kg is robot mass, $L \approx$ 0.08 cm is the distance between the center of mass and the ground contact point, $I_{pitch} \approx 1.1 \times 10^{-4}$ kg m^2 is the moment of inertia of the robot along the pitch axis about the center of mass[‡], and g = 9.81 m/s^2 is gravitational acceleration.

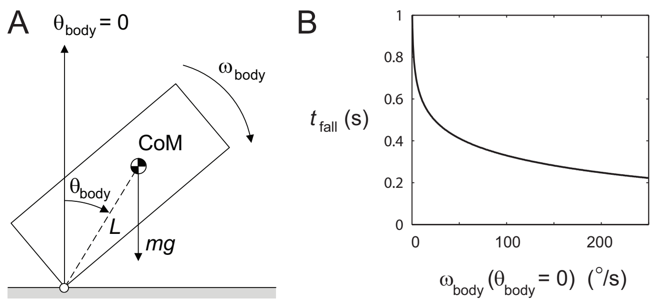

Fig. 8. Dynamic modeling of the falling phase during self-righting. (A) Schematic of a rigid body falling about a fixed pivot under gravity. (B) Model-predicted falling time as a function of body pitch angular velocity when the body was vertical.

Using this equation of motion, we numerically calculated falling time, t_{fall}, for the rigid body to rotate from vertical ($\theta_{body} = 0$) to horizontal ($\theta_{body} = 90°$) orientation, with the body pitch angular velocity when the body was vertical, $\omega_{body}(\theta_{body} = 0)$, as the initial condition. Our model predicted a decreasing t_{fall} as $\omega_{body}(\theta_{body} = 0)$ increased (Fig. 8B). This means that, the more kinetic energy the body had accumulated before reaching the vertical orientation by pushing the wings against the ground (i.e., the faster it was rotating), the more quickly it would impact the ground.

The dynamic model allowed us to understand our observations of how wing opening magnitude θ and speed ω affect righting. First, for any given θ, increasing ω resulted in an approximately proportional increase in the body pitch angular velocity when the body was vertical, i.e., $\omega_{body}(\theta_{body} = 0) \propto \omega$ when θ is constant[§]. In other words, as ω increased, the robot moved in a kinematically similar fashion but at higher speeds (as reflected by the observation of $t_{rise} \propto 1/\omega$, Fig. 5C). This means that faster wing opening reduced falling time by accelerating the body faster during the rising phase and thus injecting more kinetic energy.

Second, for any given ω, an increase (or decrease) in θ increased (or decreased) the body pitch angle θ_{body} at which the wings ceased pushing against the ground and the body started falling under gravity. As a result, the kinetic energy of the robot when the body was vertical increased (or decreased). To compensate for this change, the robot had to push more slowly (or faster) for falling time to remain unchanged. This is equivalent to shifting the model predictions of t_{fall} to the left (e.g., Fig. 5D, red curve) or right (e.g., Fig. 5D, green, cyan, blue, and dark blue curves). This means that larger wing opening magnitude reduced falling time by accelerating the body over a larger angular displacement and thus injecting more kinetic energy.

We fitted our model to experimental observations of t_{fall} and found excellent agreement (Fig. 5D). In addition, our model predicted an upper bound for t_{fall} of $\approx$ 1 s, which matched well with data, further supporting the plausibility of the model.

Our dynamic model also provides insights into the dynamics and trade-offs of animal self-righting using wings. We applied the model to the discoid cockroach and found that the measured t_{fall} were significantly shorter than predicted for falling from a vertical orientation with no initial kinetic energy [27]. This suggests that the discoid cockroach builds up substantial kinetic energy to overcome potential energy barriers and self-rights dynamically. In addition, our results that decreasing wing opening magnitude can be compensated by faster wing opening may have biological implications because muscle force depends strongly on contraction magnitude and velocity [35].

V. ASYMMETRIC RIGHTING EXPERIMENTS

In our study of the discoid cockroach self-righting using wings [27], we observed that the animal often made multiple failed attempts before it successfully righted. Although the animal is capable of opening wings by wing pitch angles as large as 90°, they often opened wings by much smaller magnitudes even when successfully self-righting. Further, the animal did not always open both wings symmetrically and pitch over the head in the sagittal plane, but often opened wings asymmetrically and rotated the body out of the sagittal plane to self-right (Fig. 9). We hypothesized that asymmetric wing opening may offer an advantage for self-righting.

Fig. 9. Self-righting of the discoid cockroach by asymmetric wing opening, resulting in asymmetric body rotation.

Our robot allowed us to test this hypothesis as we could independently control the actuation of the two wings. We

[‡] L and I_{pitch} were measured from the robot CAD model. L and $I_{pitch} + mL^2$ changed little (up to ±15%) as the wings open.

[§] $\omega_{body}(\theta_{body}) \propto \omega$ is strictly true only before wing opening ceases. However, for the range of θ tested ($80° \leq \theta \leq 140°$), the θ_{body} at which wing opening ceased ranged between $-20°$ and $20°$, within which ω_{body} did not change substantially. Therefore, $\omega_{body}(\theta_{body} = 0) \propto \omega$ approximately holds regardless of θ.

opened the left and right wings by different motor angles, θ_L and θ_R, and at different speeds, ω_L and ω_R, while always starting and stopping them in synchrony, i.e., $\theta_L/\omega_L = \theta_R/\omega_R$, with no phase lag. We recorded high-speed videos of the robot self-righting, and tested how righting probability P_{right} changed as wing opening asymmetry increased. Both θ_L and θ_R were varied between 50° and 140°, with $\omega_{L/R}$ = 50°/s when $\theta_{L/R}$ = 50°. For each combination of θ_L and θ_R, 10 trials were performed.

We observed four outcomes when the robot attempted to right using asymmetric wing opening (Fig. 10A). First, when θ_L and θ_R were both small, the robot often failed to right. Second, as θ_L or θ_R increased but were different, the robot often under-righted (see attached video): the body rotated enough to overcome the major potential energy barrier but did not fully right due to minor potential energy barriers induced by the corners and edges of the body. Third, when θ_L and θ_R were both large, the robot often succeeded in reaching the upright orientation. Finally, for some combinations of θ_L and θ_R that were different, the robot overshot after reaching an upright body orientation, resulting in over-righting (see attached video)¶. In our animal study, the discoid cockroach also showed under-righting and over-righting, but could always fully right afterwards by using legs to adjust body orientation [27]. We noted that the reduced width between the ground contact points of the two wings due to wing pitch and wing roll was essential to allow asymmetric body rotations.

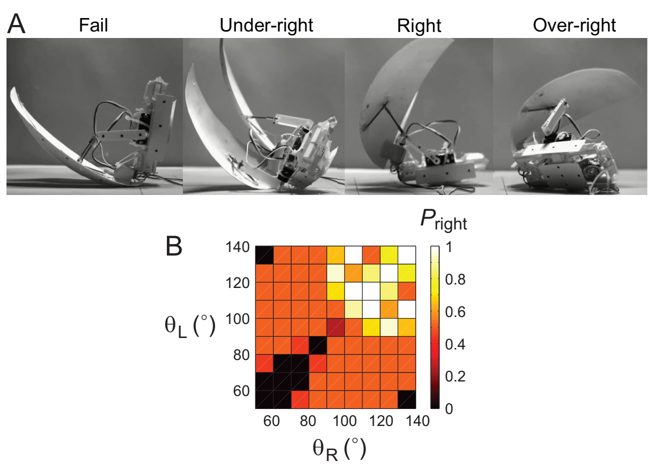

Fig. 10. Robot self-righting using asymmetric wing opening. (A) Snapshots of four righting outcomes. See text for definition of righting probability of each outcome. (B) Average righting probability as a function of left and right wing opening magnitudes, θ_L and θ_R.

We calculated the average righting probability for each combination of θ_L and θ_R, by defining righting probability of failure, under-righting, over-righting, and success as 0, 0.5, 0.5, and 1. When θ_L and θ_R were both large ($> 100°$), righting probability P_{right} was high ($> 80\%$) regardless of wing opening asymmetry (Fig. 10B, top right). However, when θ_L and θ_R were both small ($< 90°$), P_{right} was higher for asymmetric wing opening ($\approx 50\%$) than for symmetric wing opening (≈ 0) (Fig. 10B, bottom left).

These results elucidated the usefulness of asymmetric wing opening during self-righting. The animal's wing opening magnitudes are highly variable from attempt to attempt, resulting in multiple failed attempts before successful righting is achieved. As the animal fatigues during failed righting attempts, its wing opening magnitudes decrease. In this case, asymmetric wing opening becomes more advantageous because it increases the probability of righting and thus reduces the total number of attempts, time, and energy needed. In addition, asymmetric wing opening results in asymmetric body rotations, which overcome lower potential energy barriers as compared to pitching over the head [27]. Therefore, asymmetric wing opening may be an adaptation of the animal to right more quickly and economically.

VI. CONCLUSIONS & FUTURE WORK

We developed actuated wings to enable small legged robots to dynamically self-right. We demonstrated that robots can use existing body structures in novel ways to achieve new locomotor capabilities, analogous to exaptations [2] or co-opting of structures common in animals. The robot first opened its wings to push against the ground, injecting kinetic energy to overcome potential energy barriers, and then fell under gravity dynamically on its end to self-right. Our results showed that dynamic self-righting using wings benefits from larger amplitude and faster wing opening, and suggested that the discoid cockroach uses substantial kinetic energy to dynamically self-right. When animals fatigue or robots suffer power reduction or limitation, asymmetric wing opening becomes more useful because it increases righting probability and overcomes lower potential energy barriers.

Our next step is to integrate the self-righting mechanism with rounded shells to enable legged robots to both traverse obstacles [2] and self-right. We envision that our approach will help robots overcome diverse locomotor challenges and achieve life-like multi-modal locomotion in complex terrain without having to add complex, specialized structures. Furthermore, we will continue to use our self-righting robot as a physical model to better understand dynamic self-righting [36]. For example, we plan to test if body vibrations help animals access lower energy barrier locomotor pathways [1], study how legs help correct under- and over-righting [27], and explore how the topology [20] and mechanical properties [1] of terrain affect self-righting. We also need to measure ground reaction forces and develop multi-body dynamic simulations [6] to better understand the dynamics of rising phase of righting.

ACKNOWLEDGMENT

We thank Rundong Tian, David Strachan-Olson, Zach Hammond, Will Roderick, Mel Roderick, Sunny Aggarwal for initial prototypes and preliminary experiments, Kaushik Jayaram, Nate Hunt, Tom Libby, Andrew Pullin for helpful discussions, and four anonymous reviewers for helpful comments and suggestions.

¶We noted that trial-to-trial variations were higher for asymmetric wing opening than for symmetric wing opening.

References

[1] C. Li, A. O. Pullin, D. W. Haldane, H. K. Lam, R. S. Fearing, and R. J. Full, "Terradynamically streamlined shapes in animals and robots enhance traversability through densely cluttered terrain," *Bioinspiration & Biomimetics*, vol. 10, no. 4, p. 046003, 2015.

[2] S. Jay, E. S. Vrba, S. Paleobiology, N. Winter, S. J. Gould, and E. S. Vrba, "Exaptation-A Missing Term in the Science of Form," *Palaeontology*, vol. 8, no. 1, pp. 4–15, 1982.

[3] U. Saranli, M. Buehler, and D. E. Koditschek, "RHex: A Simple and Highly Mobile Hexapod Robot," *The International Journal of Robotics Research*, vol. 20, no. 7, pp. 616–631, 2001.

[4] J. E. Bares and D. Wettergreen, "Dante II : Technical Description, Results, and Lessons Learned," *The International Journal of Robotics Research*, vol. 18, no. 7, pp. 621–649, 1999.

[5] J. C. Spagna, D. I. Goldman, P.-C. Lin, D. E. Koditschek, and R. J. Full, "Distributed mechanical feedback in arthropods and robots simplifies control of rapid running on challenging terrain." *Bioinspiration & Biomimetics*, vol. 2, no. 1, pp. 9–18, 2007.

[6] C. Li, T. Zhang, and D. I. Goldman, "A Terradynamics of Legged Locomotion on Granular Media," *Science*, vol. 339, no. 6126, pp. 1408–1412, 2013.

[7] E. Guizzo and E. Ackerman, "The Hard Lessons of DARPA ' s Robotics Challenge," *IEEE Spectrum*, vol. 52, no. 8, pp. 11–13, 2015.

[8] S. Kim, J. E. Clark, and M. R. Cutkosky, "iSprawl: Design and tuning for high-speed autonomous open-loop running," *The International Journal of Robotics Research*, vol. 25, no. 9, pp. 903–912, 2006.

[9] D. W. Haldane, K. C. Peterson, F. L. G. Bermudez, and R. S. Fearing, "Animal-inspired Design and Aerodynamic Stabilization of a Hexapedal Millirobot," *IEEE International Conference on Robotics and Automation*, pp. 3279–3286, 2013.

[10] M. Kaspari and M. Weiser, "The size-grain hypothesis and interspecific scaling in ants," *Functional Ecology*, vol. 13, no. 4, pp. 530–538, 1999.

[11] U. Saranli, A. Rizzi, and D. E. Koditschek, "Model-Based Dynamic Self-Righting Maneuvers for a Hexapedal Robot," *The International Journal of Robotics Research*, vol. 23, no. 9, pp. 903–918, 2004.

[12] A. M. Johnson and D. E. Koditschek, "Legged Self-Manipulation," in *IEEE Access*, vol. 1, no. 33, 2013, pp. 310–334.

[13] P. Fiorini and J. Burdick, "The development of hopping capabilities for small robots," *Autonomous Robots*, vol. 2, no. 14, pp. 239–254, 2003.

[14] M. Kovac, M. Schlegel, J.-C. Zufferey, and D. Floreano, "Steerable miniature jumping robot," *Autonomous Robots*, vol. 28, no. 3, pp. 295–306, dec 2009.

[15] E. Beyer and M. Costello, "Performance of a Hopping Rotochute," *International Journal of Micro Air Vehicles*, vol. 1, no. 2, pp. 121–137, 2009.

[16] E. Tunstel, "Evolution of Autonomous Self-Righting Behaviors for Articulated Nanorovers," *Artificial Intelligence, Robotics and Automation in Space*, vol. 440, pp. 341–346, 1999.

[17] H. Schempf, E. Mutschler, C. Piepgras, J. Warwick, B. Chemel, S. Boehmke, W. Crowley, R. Fuchs, and J. Guyot, "Pandora: autonomous urban robotic reconnaissance system," *IEEE International Conference on Robotics and Automation*, vol. 3, pp. 2315–2321, 1999.

[18] C. C. Kessens, D. C. Smith, and P. R. Osteen, "A Framework for Autonomous Self-Righting of a Generic Robot on Sloped Planar Surfaces," *IEEE International Conference on Robotics and Automation*, pp. 4724–4729, 2012.

[19] A. Kossett and N. Papanikolopoulos, "A robust miniature robot design for land/air hybrid locomotion," *IEEE International Conference on Robotics and Automation*, pp. 4595–4600, 2011.

[20] S. Peng, X. Ding, F. Yang, and K. Xu, "Motion planning and implementation for the self-recovery of an overturned multi-legged robot," *Robotica*, vol. 5, pp. 1–14, 2015.

[21] A. Klaptocz, L. Daler, A. Briod, J.-c. Zufferey, and D. Floreano, "An Active Uprighting Mechanism for Flying Robots," *IEEE Transactions on Robotics*, vol. 28, no. 5, pp. 1152–1157, 2012.

[22] G. Krummel, K. N. Kaipa, and S. K. Gupta, "A Horseshoe Crab Inspired Surf Zone Robot with Righting Capabilities," in *ASME International Design Engineering Technical Conferences and Computers and Information in Engineering Conference*, 2014, p. V05AT08A010.

[23] M. Yim, B. Shirmohammadi, J. Sastra, M. Park, M. Dugan, and C. J. Taylor, "Towards robotic self-reassembly after explosion," *IEEE/RSJ International Conference on Intelligent Robots and Systems*, pp. 2767–2772, 2007.

[24] G. Zong, Z. Deng, and W. Wang, "Realization of a modular reconfigurable robot for rough terrain," *IEEE International Conference on Mechatronics and Automation*, vol. 2006, pp. 289–294, 2006.

[25] P. Ben-Tzvi, A. a. Goldenberg, and J. W. Zu, "Design, simulations and optimization of a tracked mobile robot manipulator with hybrid locomotion and manipulation capabilities," *IEEE International Conference on Robotics and Automation*, pp. 2307–2312, 2008.

[26] H. Tsukagoshi, M. Sasaki, A. Kitagawa, and T. Tanaka, "Design of a higher jumping rescue robot with the optimized pneumatic drive," in *IEEE International Conference on Robotics and Automation*, 2005, pp. 1276–1283.

[27] C. Li, T. Wohrl, H. K. Lam, and R. J. Full, "Fast, flipping cockroaches: dynamic, self-righting behavior," in *Integrative and Comparative Biology*, vol. 55, 2015, p. E111.

[28] R. Full, A. Yamauchi, and D. Jindrich, "Maximum single leg force production: cockroaches righting on photoelastic gelatin," *The Journal of experimental biology*, vol. 198, no. 12, pp. 2441–2452, 1995.

[29] L. Frantsevich, "Righting kinematics in beetles (Insecta: Coleoptera)." *Arthropod structure & development*, vol. 33, no. 3, pp. 221–35, 2004.

[30] G. Domokos and P. L. Várkonyi, "Geometry and self-righting of turtles." *Proceedings of The Royal Society of London B: Biological Sciences*, vol. 275, no. 1630, pp. 11–7, 2008.

[31] J. S. Young, L. S. Peck, and T. Matheson, "The effects of temperature on walking and righting in temperate and Antarctic crustaceans," *Polar Biology*, vol. 29, no. 11, pp. 978–987, 2006.

[32] J. Brackenbury, "A novel method of self-righting in the springtail Sminthurus viridis (Insecta : Collembola)," *Journal of Zoology*, vol. 222, pp. 117–119, 1990.

[33] C. C. Kessens, C. T. Lennon, and J. Collins, "A metric for self-rightability and understanding its relationship to simple morphologies," *IEEE/RSJ International Conference on Intelligent Robots and Systems*, pp. 3699–3704, 2014.

[34] A. M. Hoover and R. S. Fearing, "Fast scale prototyping for folded millirobots," *IEEE International Conference on Robotics and Automation*, pp. 886–892, 2008.

[35] M. H. Dickinson, C. T. Farley, R. J. Full, M. A. R. Koehl, R. Kram, and S. Lehman, "How animals move: An integrative view," *Science*, vol. 288, no. 5463, pp. 100–106, 2000.

[36] J. Aguilar, T. Zhang, F. Qian, M. Kingsbury, B. McInroe, N. Mazouchova, C. Li, R. Maladen, C. Gong, M. Travers, R. L. Hatton, H. Choset, P. B. Umbanhowar, and D. I. Goldman, "A review on locomotion robophysics: the study of movement at the intersection of robotics, soft matter and dynamical systems," *Reports on Progress in Physics*, 2016.